DOI: 10.1002/chem.200901105

Change in the Site of Electron-Transfer Reduction of a Zinc–Quinoxalinoporphyrin/Gold–Quinoxalinoporphyrin Dyad by Binding of Scandium Ions and the Resulting Remarkable Elongation of the Charge-Shifted-State Lifetime

Kei Ohkubo,[a] Rachel Garcia,[b] Paul J. Sintic,[c] Tony Khoury,[c] Maxwell J. Crossley,*[c] Karl M. Kadish,*[b] and Shunichi Fukuzumi*[a]

Abstract: The site of electron-transfer reduction of $AuPQ^+$ (PQ = 5,10,15,20-tetrakis(3,5-di-*tert*-butylphenyl)quinoxalino[2,3−*b*′]porphyrin) and $AuQPQ^+$ (QPQ = 5,10,15,20-tetrakis(3,5-di-*tert*-butylphenyl)bisquinoxalino[2,3-*b*′:12,13-*b*″]porphyrin) is changed from the Au^{III} center to the quinoxaline part of the PQ macrocycle in the presence of Sc^{3+} in benzonitrile because of strong binding of Sc^{3+} to the two nitrogen atoms of the quinoxaline moiety. Strong binding of Sc^{3+} to the corresponding nitrogen atoms on the quinoxaline unit of ZnPQ also occurs for the neutral form. The effects of Sc^{3+} on the photodynamics of an electron donor–acceptor compound containing a linked Zn^{II} and Au^{III} porphyrin ($[ZnPQ–AuPQ]PF_6$) have been examined by femto- and nanosecond laser flash photolysis measurements. The observed transient absorption bands at 630 and 670 nm after laser pulse irradiation in the absence of Sc^{3+} in benzonitrile are assigned to the charge-shifted (CS) state ($ZnPQ^{\bullet+}$–AuPQ). The CS state decays through back electron transfer (BET) to the ground state rather than to the triplet excited state. The BET rate was determined from the disappearance of the absorption band due to the CS state. The decay of the CS state obeys first-order kinetics. The CS lifetime was determined to be 250 ps in benzonitrile. Addition of Sc^{3+} to a solution of ZnPQ–$AuPQ^+$ in benzonitrile caused a drastic lengthening of the CS lifetime that was determined to be 430 ns, a value 1700 times longer than the 250 ps lifetime measured in the absence of Sc^{3+}. Such remarkable prolongation of the CS lifetime in the presence of Sc^{3+} results from a change in the site of electron transfer from the Au^{III} center to the quinoxaline part of the PQ macrocycle when Sc^{3+} binds to the quinoxaline moiety, which decelerate BET due to a large reorganization energy of electron transfer. The change in the site of electron transfer was confirmed by ESR measurements, redox potentials, and UV/Vis spectra of the singly reduced products.

Keywords: donor–acceptor systems · electron transfer · macrocycles · porphyrinoids · scandium

[a] Dr. K. Ohkubo, Prof. Dr. S. Fukuzumi
Department of Material and Life Science
Graduate School of Engineering
Osaka University and
SORST (JST)
2–1 Yamada-oka, Suita, Osaka 565-0871 (Japan)
Fax: (+81) 6-6879-7370
E-mail: fukuzumi@chem.eng.osaka-u.ac.jp

[b] R. Garcia, Prof. Dr. K. M. Kadish
Department of Chemistry, University of Houston
Houston, TX 77204-5003 (USA)
Fax: (+1) 713-743-2745
E-mail: kkadish@uh.edu

[c] Dr. P. J. Sintic, Dr. T. Khoury, Prof. Dr. M. J. Crossley
School of Chemistry, The University of Sydney
NSW 2006 (Australia)
Fax: (+61) 2-9351-3329
E-mail: m.crossley@chem.usyd.edu.au

Supporting information for this article is available on the WWW under http://dx.doi.org/10.1002/chem.200901105.

Introduction

In the photosynthetic reaction center, charge separation (CS) is faster than charge recombination (CR).[1] The fast CS is made possible due to a large CR driving force that is located in the Marcus inverted region,[2] in which the driving force ($-\Delta G_{ET}$; ET = electron transfer) is larger than the reorganization energy of electron transfer (λ), that is, $-\Delta G_{ET} > \lambda$. The CR rate decreases as the driving force of electron transfer increases in the Marcus inverted region, whereas the CS rate increases in the Marcus normal region ($-\Delta G_{ET} < \lambda$).[2] In such a case, the smaller the λ value, the faster the CS rate and the slower becomes the CR rate.[2] Thus, the same strategy as used in natural photosynthesis has so far been chosen to optimize the efficiency of the charge separation processes in biomimetic electron donor–acceptor ensembles, that is, the use of components which

have small reorganization energies of electron transfer in order to accelerate the forward electron transfer in the Marcus normal region, and to decelerate the back electron transfer in the Marcus inverted region.[3–10]

A totally opposite approach to attain long-lived CS states would be to use a component that has a large λ value, which may result in slow CR in the Marcus normal region ($-\Delta G_{ET} < \lambda$). In such a case, the CS driving force should be much larger than the CR driving force to make the CS rate faster than the CR rate. Metalloporphyrins, which are frequently used in photosynthetic models for light-harvesting and electron-donor molecules, have relatively small λ values,[3–10] and thus these metallomacrocycles cannot be used by themselves as the component with a large λ value.

On the other hand, extremely large λ values have commonly been associated with ET reduction of electron acceptors when metal ions bind strongly to radical anions of electron acceptors.[11–18] The scandium ion (Sc^{3+}) is known to be most effective for binding to radical anions.[15–18] Thus, if metal-ion binding sites are introduced into metalloporphyrins, they would be good candidates as a component in the construction of electron donor–acceptor (D–A) dyads that can afford long-lived CS states with large λ values due to strong binding of metal ions. In this context, the fusion of a quinoxaline group to the β,β′-pyrrolic position of the porphyrin macrocycle[19,20] merits special attention, as it can act as a metal-ion binding site. The quinoxaline group also leads to easier reduction and a greater degree of delocalization throughout the molecule,[19,20] resulting in more effective electron transfer of the entire complex.

We previously reported the initial site of electron transfer in "simple" Au^{III} porphyrins (AuP^+) to be at the central metal ion, giving a Au^{II} complex when the measurement was carried out in nonaqueous solvents such as benzonitrile, CH_2Cl_2, pyridine, or THF.[21] Gold(III) quinoxalinoporphyrins ($AuPQ^+$) were also shown to undergo reduction at the central metal ion to give the gold(II)–porphyrin complex,[22] overturning the long-held assumption that reduction of such complexes only occurs at the macrocycle.[23–25] The fused quinoxaline group on the porphyrin macrocycle is typically reduced at potentials more negative than −1.9 V versus SCE as compared to the reversible reduction of quinoxaline itself which occurs at $E_{1/2} = -1.60$ V in THF containing 0.1 M TBAP.[26] We have also reported the synthesis and photoinduced electron-transfer dynamics of electron D–A linked systems involving $AuPQ^+$.[27] Gold(III)–porphyrin complexes have frequently been used as electron acceptors in donor–acceptor ensembles due to their ability to be easily reduced.[28–34] However, neither the effect of metal ions on the ET reduction of quinoxalinoporphyrins, nor those on the photoinduced electron transfer of D–A linked systems involving $AuPQ^+$, have so far been investigated.

This is now undertaken in the present study in which the effect of scandium ion (Sc^{3+}) on the electron-transfer reduction of gold(III)–quinoxalino- and –bisquinoxalinoporphyrin complexes ($AuPQ^+$ and $AuQPQ^+$) is elucidated. As will be shown, there is a dramatic effect of Sc^{3+} on the electron-transfer reduction of $AuPQ^+$ and $AuQPQ^+$, which not only changes the site of electron transfer from the Au^{III} metal to the fused quinoxaline part of the PQ macrocycle, but also leads to a remarkable elongation of the lifetime in the charge-shifted state of a ZnPQ–AuPQ dyad in benzonitrile due to the strong binding of Sc^{3+} to the ZnPQ and $AuPQ^+$ moieties.

The present study provides an alternative and convenient way to attain long-lived CS states by the simple binding of metal ions to porphyrin-based donor–acceptor dyads. The investigated compounds, ZnPQ, $[AuPQ]PF_6$, $[AuQPQ]PF_6$, and $[ZnPQ–AuPQ]PF_6$, are shown here.

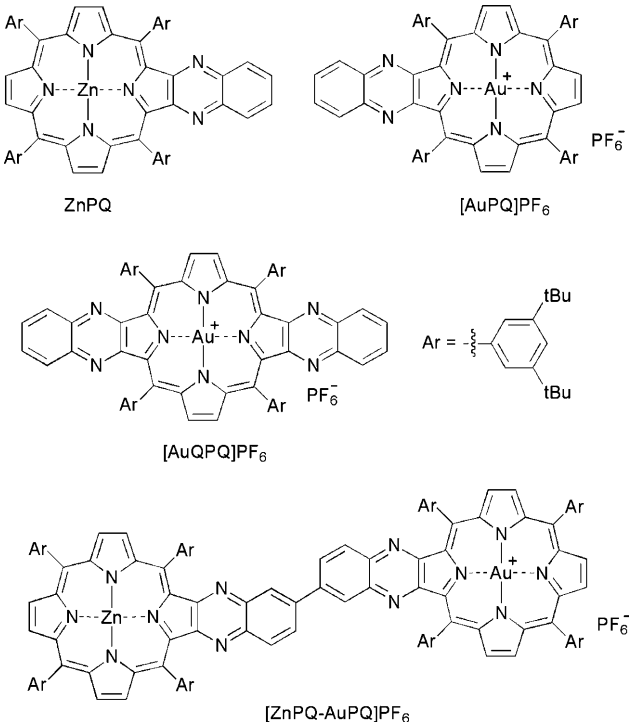

Results and Discussion

Positive shift of one-electron reduction potential of $AuPQ^+$: A cyclic voltammogram of $[AuPQ]PF_6$ in PhCN before and after the addition of two equivalents of $Sc(OTf)_3$ is shown in Figure 1. Before the addition of Sc^{3+}, the porphyrin exhibits three reductions, the first of which is metal-centered. This behavior is comparable with that of other Au^{III}–porphyrins previously examined by our groups.[21,22] No oxidations are observed for gold quinoxalinoporphyrins up to positive range of the PhCN solvent (about 1.8 V vs SCE).

The second and third reductions of $[AuPQ]PF_6$ afford the Au^{II}–porphyrin π-radical anion and the porphyrin dianion, respectively. The potential separation between the first and second one-electron reduction of $[AuPQ]PF_6$ is 500 mV, and the separation between the second and the third processes is 680 mV in PhCN. These latter values of $\Delta E_{1/2}$ are comparable to what was reported for $[AuP]PF_6$ under the same solu-

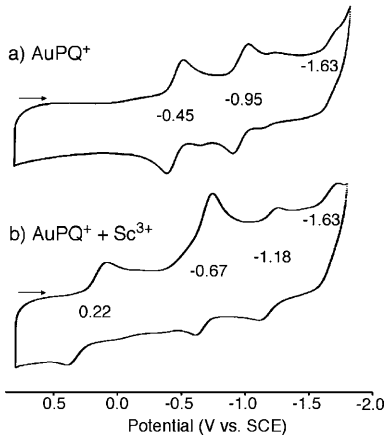

Figure 1. Cyclic voltammograms of $[AuPQ]PF_6$ (3.7×10^{-4} M) a) before and b) after the addition of $Sc(OTf)_3$ (7.4×10^{-4} M) to a PhCN solution containing 0.10 M $TBAPF_6$.

tion conditions.[21] All three processes are positively shifted by 210 mV upon going from $[AuP]PF_6$ to $[AuPQ]PF_6$, consistent with what has been reported for the other quinoxalinoporphyrins.[19,20,22,26]

Four redox processes are observed for $[AuPQ]PF_6$ in PhCN containing two equivalents of $Sc(OTf)_3$ (Figure 1b), the first of which occurs at $E_{1/2}=+0.22$ V, which is significantly shifted to the positive direction as compared to that in the absence of $Sc(OTf)_3$.[35] The following two reversible reduction waves at $E_{1/2}=-0.67$ and -1.18 V and the reduction peak at $E_p=-1.63$ V, are potentials almost identical to the $E_{1/2}$ values for the reduction of $[AuP]PF_6$ in PhCN not containing Sc^{3+}.[21,36] The large positive shift in the first reduction potential of $[AuPQ]PF_6$ allows the electron-transfer reduction to be carried out by decamethylferrocene (Fc*) in the presence of Sc^{3+} (vide infra).

No electron transfer from Fc* to $[AuPQ]PF_6$ occurs in the absence of Sc^{3+}, because the electron transfer is highly endergonic judging from the one-electron oxidation potential of Fc* ($E_{ox}=-0.11$ V vs. SCE)[37,38] and the one-electron reduction potential of $[AuPQ]PF_6$ ($E_{red}=-0.45$ V vs. SCE). However, the addition of Sc^{3+} to a PhCN solution of $[AuPQ]PF_6$ in the presence of Fc* results in a homogenous electron transfer from Fc* to $[AuPQ]PF_6$ to produce Fc^{*+} and $AuPQ^{\bullet-}$ as shown in Figure 2. Several isosbestic points are observed, and the 418 and 515 nm bands of the product can be compared with the spectrum of the same Au^{III}–porphyrin not having the fused quinoxaline group, that is, $[AuP]PF_6$ in PhCN.[21]

There is also a broad absorption band at 790 nm in the one-electron reduced product, and this can be assigned to the decamethylferricenium cation (Fc^{*+}: $\lambda_{max}=790$ nm, $\varepsilon_{max}=240\,M^{-1}cm^{-1}$),[37,38] which would be overlapped with any long-wavelength absorptions of AuPQ. Such long-wavelength absorption extending into the NIR region is diagnostic of the absorption band due to the PQ π-radical anion, and clearly indicates that the site of the electron-transfer reduction of $[AuPQ]PF_6$ is changed from the Au^{III} metal in

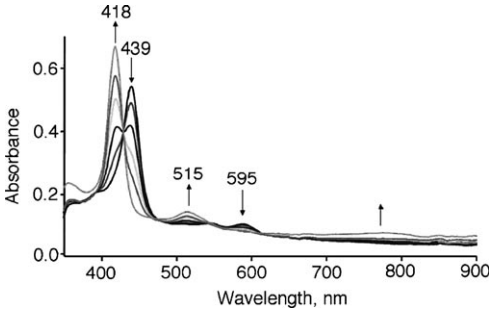

Figure 2. UV/Vis spectral change upon addition of $Sc(OTf)_3$ ($0–2.8\times10^{-5}$ M) to a solution of $[AuPQ]PF_6$ in PhCN (1.4×10^{-5} M) in the presence of Fc* (1.7×10^{-3} M).

the absence of Sc^{3+} to the macrocycle, and, more specifically, to the quinoxaline part of the compound as discussed in detail in later sections of the manuscript. It is significant to point out that the UV/Vis spectrum of the electrochemically generated $Au^{II}PQ$[22] is quite different than the spectrum of the chemically reduced product in Figure 2.

The titration curve in Figure 3a, illustrating a plot of absorbance at 439 nm due to AuPQ versus $[Sc^{3+}]/[AuPQ^+]$, shows an end point at $[Sc^{3+}]/[AuPQ^+]=2$, thus indicating

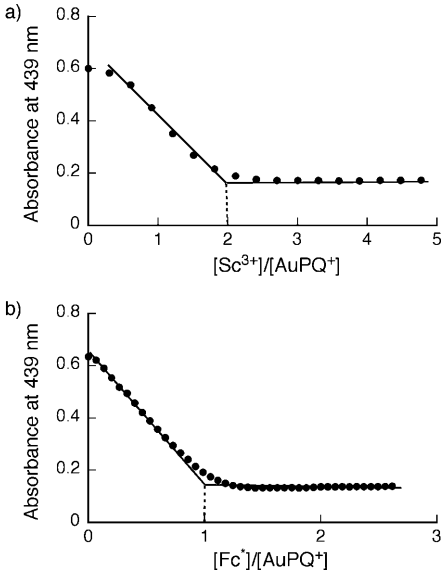

Figure 3. Plots of a) absorbance at 439 nm for $[AuPQ]PF_6$ versus $[Sc^{3+}]/[AuPQ^+]$ ratio with a fixed concentration of Fc* (1.65×10^{-4} M) and b) absorbance at 439 nm versus $[Fc^*]/[AuPQ^+]$ with a fixed concentration of Sc^{3+} (7.12×10^{-4} M) in electron transfer from Fc* to $[AuPQ]PF_6$ (1.37×10^{-5} M) in the presence of Sc^{3+} in PhCN.

that two Sc^{3+} ions are required for the electron-transfer reduction of $[AuPQ]PF_6$ by Fc*. The one-electron reduction of $[AuPQ]PF_6$ is confirmed by the titration curve in Figure 3b, in which the plot of absorbance at 439 nm due to $AuPQ^+$ versus $[Fc^*]/[AuPQ^+]$ exhibits an end point at $[Fc^*]/[AuPQ^+]=1$. It should be emphasized that the spectral titra-

tion of a solution of $AuPQ^+$ in PhCN with Sc^{3+} (see the Supporting Information Figure S1) indicates that two Sc^{3+} ions bind to $[AuPQ]PF_6$ prior to the electron-transfer reduction. Judging from the spectral titration in Figure S1, the formation of the 1:2 complex between $AuPQ^+$ and Sc^{3+} is quantitative when the binding constant is too large to be determined accurately.

When $AuPQ^+$ is replaced by $AuQPQ^+$ containing two quinoxaline units, a similar spectral change is observed for the electron-transfer reduction by Fc* as shown in Figure 4a. In this case, however, a two-electron reduction of $AuQPQ^+$ by Fc* occurs as indicated by the spectral titration data in Figure 4b, in which four equivalents of Sc^{3+} ions are required for the reaction (see the Supporting Information Figure S2).

The number of Sc^{3+} ions required for the electron-transfer reduction of $AuPQ^+$ and $AuQPQ^+$ corresponds to the total number of nitrogen atoms on the quinoxaline units, that is, two and four for $AuPQ^+$ and $AuQPQ^+$, respectively. Thus, the electron-transfer reductions of $AuPQ^+$ and $AuQPQ^+$ are made possible by binding of Sc^{3+} to the nitrogen atoms of the quinoxaline units of $AuPQ^+$ and $AuQPQ^+$, as shown in Scheme 1. The site of electron-transfer reduction of $AuPQ^+$ and $AuQPQ^+$ is not the Au^{III} center but the fused quinoxaline group on the compound, which binds with Sc^{3+} at its nitrogen atoms. Additional proof that Au^{III} is not reduced is given by the fact that similar spectral changes are observed for the electron-transfer reduction of ZnPQ by Fc* in the presence of Sc^{3+} (see the Supporting Information Figure S3).

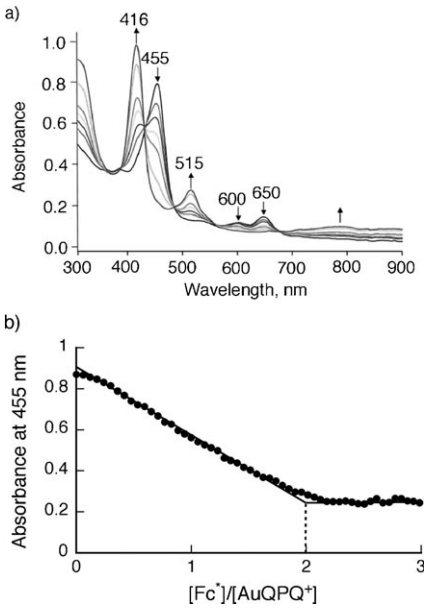

Figure 4. a) UV/Vis spectral change upon addition of Fc* ($0–2.8\times10^{-5}$ M) to a solution of $AuQPQ^+$ in PhCN (1.37×10^{-5} M) in the presence of Sc^{3+} (7.12×10^{-4} M). b) Absorbance at 455 nm versus $[Fc^*]/[AuPQ^+]$ with a fixed concentration of Sc^{3+} (7.12×10^{-4} M) in electron transfer from Fc* to $AuQPQ^+$ (1.37×10^{-5} M) in the presence of Sc^{3+} in PhCN.

ESR measurements of the electron-transfer products also confirm a change in the site of electron transfer, from the Au^{III} metal of $AuPQ^+$ in the absence of Sc^{3+}, to the fused quinoxaline unit in the presence of Sc^{3+}. Figure 5 shows an

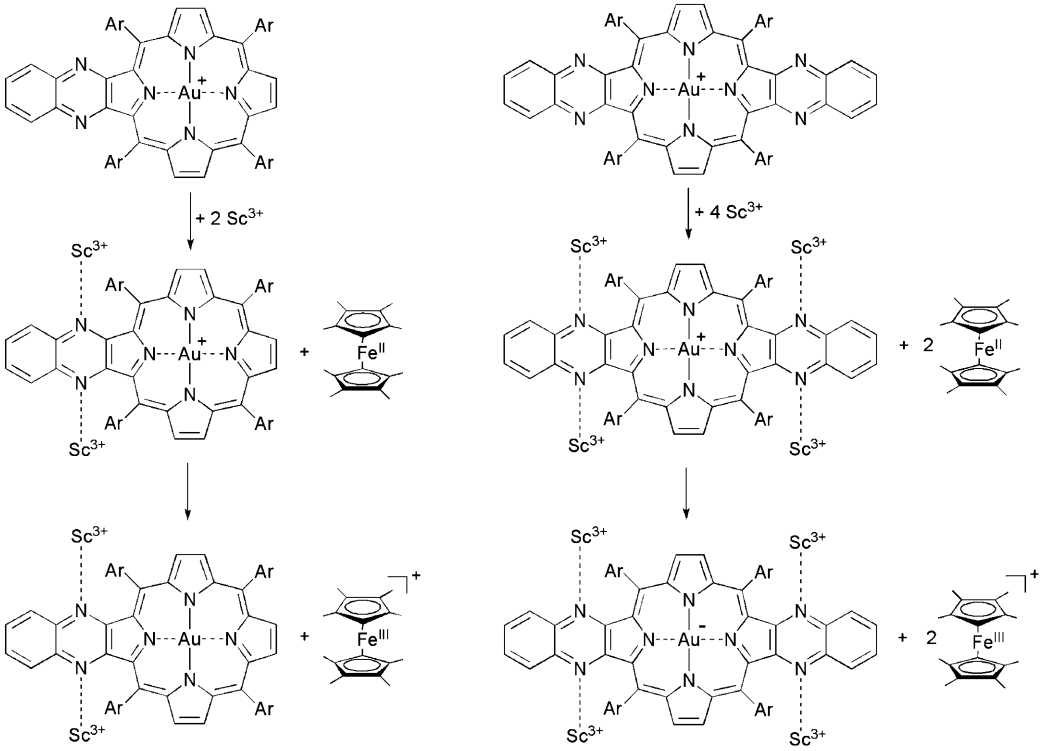

Scheme 1. Electron-transfer reduction of $AuPQ^+$ (left) and $AuQPQ^+$ (right) with decamethylferrocene in the presence of $Sc(OTf)_3$.

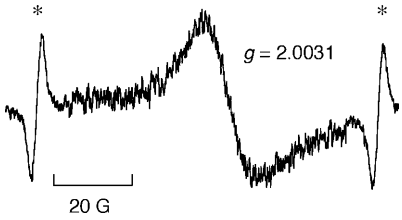

Figure 5. ESR spectrum for the products of electron-transfer reduction of $AuPQ^+$ (7.0×10^{-4} M) by Fc* (7.0×10^{-4} M) in PhCN containing $Sc(OTf)_3$ (5.0×10^{-3} M) at 298 K. Asterisk denotes Mn^{2+} marker.

ESR spectrum of the products formed after electron-transfer reduction of $AuPQ^+$ by Fc* in the presence of Sc^{3+} in PhCN. The g value of 2.0031 is consistent with the reported g value of the Sc^{3+} complex of the acridine radical anion ($g=2.0031$), in which Sc^{3+} binds to the nitrogen of the acridine radical anion.[17a] The measured ESR signal due to the one-electron reduced species of the quinoxaline unit is in sharp contrast to the broad ESR signal having a much larger g value (2.06) for the Au^{II}–porphyrin observed after the one-electron reduction of $AuPQ^+$ by the naphthalene radical anion.[22]

The change in site of the electron-transfer reduction of $AuPQ^+$ resulting from binding of Sc^{3+} to the nitrogen of the quinoxaline unit is also supported by DFT calculations. Figure 6 (top) shows the LUMO also changed to the fused quinoxaline unit upon protonation. When Sc^{3+} binds to the nitrogen atoms of the quinoxaline unit of $AuPQ^+$, however, the LUMO orbital is localized on the Sc^{3+} nucleus. Thus, the solvation orbital initially delocalized on the Au^{III} metal, but also to a lesser extent on the macrocycle, whereas Figure 6 (bottom) shows that the LUMO orbitals of the Sc^{3+} and the counter anion (OTf^-) may be important factors in determining the site of electron transfer.[39]

If the change in site of electron-transfer reduction of $Au^{III}PQ$ results from the stronger binding of Sc^{3+} to the quinoxaline unit of $Au^{III}PQ^{\bullet-}$ (one-electron reduced species) as compared to that of $Au^{III}PQ$, the one-electron reduction potential of quinoxaline should also exhibit a large positive shift. This is indeed the case, as shown in Figure 7 in which $E_{1/2}$ (−1.66 V vs. SCE) is shifted to a more positive potential: one at $E_{1/2}=0.25$ V, and the other at $E_{1/2}=-0.17$ V versus SCE in the presence of two equivalents of Sc^{3+}. The first quasi-reversible process at 0.25 V is located at nearly the same potential as for $AuPQ^+$ reduction in PhCN containing two equivalents of Sc^{3+} (Figure 1).

Reorganization energy of electron transfer for reduction of $AuPQ^+$: The large positive shift in the one-electron potential of $AuPQ^+$, from −0.45 to +0.22 V versus SCE, caused by the much stronger binding to $PQ^{\bullet-}$ than to PQ (Figure 1) makes the electron transfer from Fc* to $AuPQ^+$ occur as shown in Figure 2. No electron transfer from 1,1′-dimethylferrocene (Me_2Fc; $E_{ox}=0.26$ V vs. SCE) to $AuPQ^+$ occurs in PhCN at 298 K, because the free energy change of electron transfer (ΔG_{et}) is largely positive (0.71 eV). The ΔG_{et} value for electron transfer from Me_2Fc to $AuPQ^+$ is changed by the addition of Sc^{3+} (+0.04 eV), judging from the one-electron reduction potential of the $AuPQ^+/(Sc^{3+})_2$ species ($E_{red}=0.22$ V vs. SCE). Thus, in the presence of two equivalents of Sc^{3+}, an efficient electron transfer from Me_2Fc to $AuPQ^+/(Sc^{3+})_2$ occurred to yield $AuPQ^{\bullet}/(Sc^{3+})_2$ and Me_2Fc^+ [Eq. (1)].

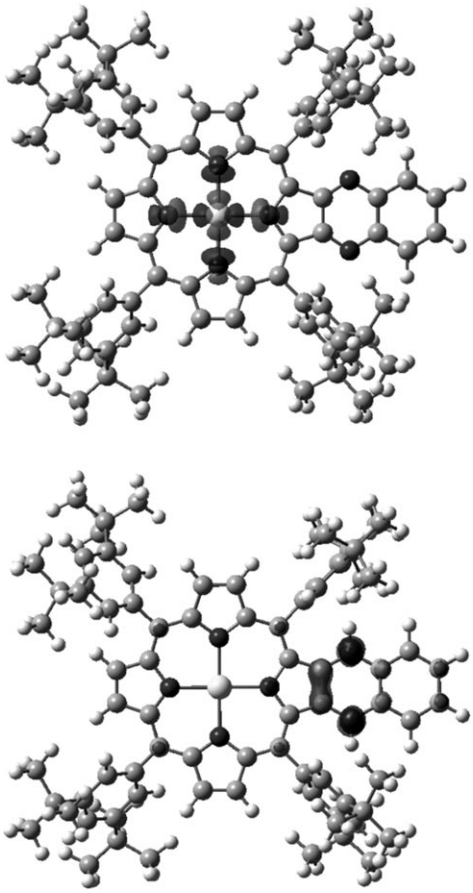

Figure 6. LUMO orbitals of $AuPQ^+$ (top) and diprotonated $AuPQ^+$ (bottom) calculated by the DFT method at the B3LYP/lanl2dz level.

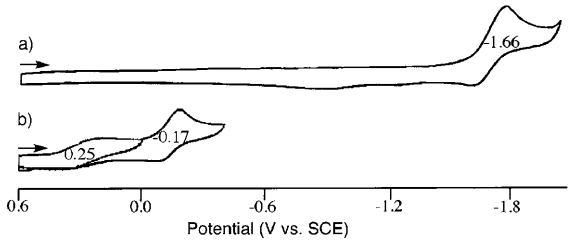

Figure 7. Cyclic voltammograms of a) quinoxaline (1.18×10^{-3} M) in PhCN, $TBAPF_6$ (0.1 M) only and b) the same solution in the presence of $Sc(OTf)_3$ (2.45×10^{-3} M).

$$Me_2Fc + AuPQ^+/(Sc^{3+})_2 \rightarrow Me_2Fc^+ + AuPQ^{\bullet}/(Sc^{3+})_2 \quad (1)$$

Figure 8a shows UV/Vis spectral changes as a function of time for the electron transfer from Me_2Fc to $AuPQ^+$ in the

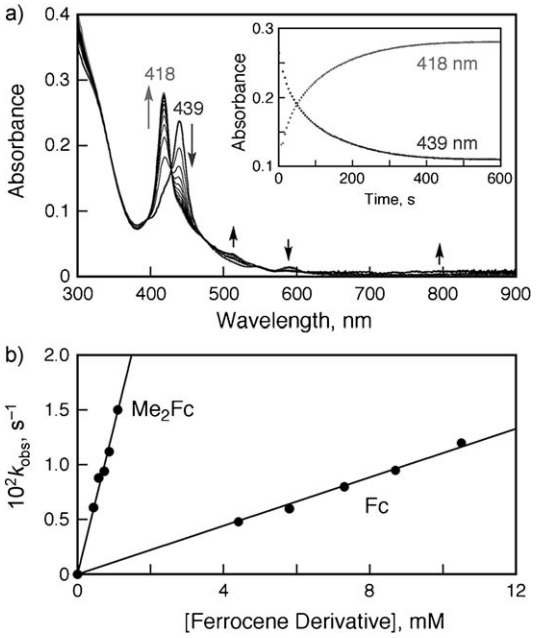

Figure 8. a) UV/Vis spectral change in electron transfer from Me_2Fc (5.8×10^{-4} M) to $AuPQ^+$ (5.8×10^{-5} M) in the presence of $Sc(OTf)_3$ (1.1×10^{-3} M) in deaerated PhCN at 298 K. Inset: Decay and rise time profiles at 418 nm and 439 nm. b) Plots of pseudo-first-order rate constants versus concentration of Me_2Fc and Fc in electron transfer from Me_2Fc (5.8×10^{-4} M) to $AuPQ^+$ (5.8×10^{-5} M) in the presence of $Sc(OTf)_3$ (1.1×10^{-3} M).

presence of Sc^{3+} in PhCN. The decay of $AuPQ^+$ ($\lambda_{max}=$ 439 nm) and the formation of $AuPQ^{\bullet}$ ($\lambda_{max}=418$ nm) are also shown in the inset of Figure 8a. The decay and rise time profiles obey pseudo-first-order kinetics, and the pseudo-first-order rate constant (k_{obs}) increases linearly with increasing concentration of Me_2Fc (Figure 8b). The observed second-order rate constant (k_{et}) is determined as $13\,M^{-1}s^{-1}$. The dependence of the k_{et} value on the ΔG_{et} value for outer-sphere electron transfer has been well-established by Marcus as given by Equation (2), in which λ is the reorganization energy of electron transfer, k_B is the Boltzmann constant and Z is the collision frequency, taken as $1\times10^{11}\,M^{-1}s^{-1}$.[2]

$$k_{et} = Z\exp[-(\lambda/4)(1+\Delta G_{rt}/\lambda)^2/k_B T] \quad (2)$$

The λ value is determined as 2.26 eV for the electron transfer from Me_2Fc to $AuPQ^+/(Sc^{3+})_2$ from the k_{et} and ΔG_{et} values using Equation (3), which is derived from Equation (2).

$$\lambda = -\Delta G_{et} - 2RT\ln(k_{et}/Z) + [\{\Delta G_{et} + 2k_B T\ln(k_{et}/Z)\}^2 - (\Delta G_{et})^2]^{1/2} \quad (3)$$

Virtually the same λ value (2.29 eV) is obtained from the k_{et} ($1.1\,M^{-1}s^{-1}$) and ΔG_{et} (0.15 eV) values of electron transfer from Fc ($E_{ox}=0.37$ V vs. SCE) to $AuPQ^+/(Sc^{3+})_2$. The λ value obtained for electron-transfer reduction of $AuPQ^+/(Sc^{3+})_2$ is significantly larger than the reported λ values of metal-centered electron-transfer reactions of gold–porphyrin ($\lambda=\approx1.23$ eV).[22]

Photoinduced electron transfer in ZnPQ–$AuPQ^+$ dyad in the presence of Sc^{3+}: We previously reported the formation of a long-lived CS state of the ZnPQ–$AuPQ^+$ dyad in non-polar solvents such as cyclohexane.[27a] However, the long CS lifetime (10 μs) in cyclohexane becomes much shorter in PhCN (250 ps).[27b] Such a short-lived CS state could only be measured by using femtosecond laser flash photolysis. The short CS lifetime in PhCN results from the large solvent reorganization energy for the back electron transfer in contrast to the much smaller solvent reorganization energy in cyclohexane. This is because the larger the reorganization energy, the faster the rate of back electron transfer, as expected from the Marcus theory of electron transfer, provided that the driving force of back electron transfer is larger than the reorganization energy of electron transfer.[2] This region is referred to as the Marcus inverted region.[2]

Time-resolved transient absorption spectra of ZnPQ–$AuPQ^+$ in the absence and presence of Sc^{3+} were measured by femtosecond laser photolysis. A transient absorption spectrum observed after the femtosecond laser pulse excitation of a solution of ZnPQ–$AuPQ^+$ in PhCN in the absence of Sc^{3+} is shown in Figure 9a. The observed transient absorption band at 670 nm and the shoulder at 760 nm at 1 ps after femtosecond laser excitation agree with those observed in the one-electron oxidation of ZnPQ to $ZnPQ^{\bullet+}$ (Supporting Information S4a). There is no significant absorption at 600–800 nm due to $Au^{II}PQ$ and thus the observed transient absorption spectrum in Figure 9a indicates that electron transfer from ^{1}ZnPQ* to $AuPQ^+$ occurs to afford $ZnPQ^{\bullet+}$–$Au^{II}PQ$.[27a] The first fast-decay component at 590 nm with the rate constant of $3.7\times10^{12}\,s^{-1}$ (lifetime of 270 fs) agrees with the rise in rate at 760 nm for the formation of $ZnPQ^{\bullet+}$ (inset of Figure 9b). This process corresponds to the electron transfer from the singlet excited state of ZnPQ (^{1}ZnPQ*) to $AuPQ^+$ to form the charge-shifted (CS) state, $ZnPQ^{\bullet+}$–$Au^{II}PQ$. The second component with the rate constant of $6.7\times10^{10}\,s^{-1}$ (lifetime of 15 ps) seen in Figure 9b corresponds to the electron transfer from ZnPQ to the triplet excited state of $AuPQ^+$ ($^3AuPQ^{+}$*), in which $^3AuPQ^{+}$* is produced by extremely fast intersystem crossing of the $^1AuPQ^{+}$* moiety upon the 410 nm laser pulse illumination of the $AuPQ^+$ unit.[40] The ratio of laser excitation of the ZnPQ and $AuPQ^+$ units is 15:1, determined from their absorption coefficients at 410 nm. The final slow component with the rate constant of $4.0\times10^{9}\,s^{-1}$ (lifetime of 250 ps) corresponds to the back electron transfer from $Au^{II}PQ$ to $ZnPQ^{\bullet+}$ to the ground state.

In contrast to the short-lived CS state of ZnPQ–$AuPQ^+$ in the absence of Sc^{3+} in PhCN (Figure 9), the transient absorption spectrum observed after the femtosecond laser pulse excitation of a solution of ZnPQ–$AuPQ^+$ in PhCN in the presence of Sc^{3+} (5 mM) remains the same at 3000 ps, as shown in Figure 10a (dark gray circles). The observed transient absorption bands at 630 nm and the shoulder at 670 nm

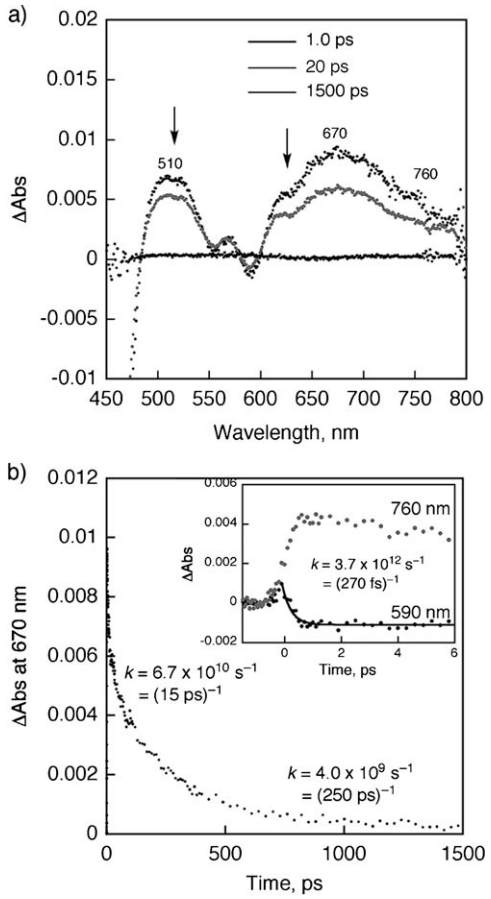

Figure 9. a) Transient absorption spectra of ZnPQ–AuPQ$^+$ in the absence of Sc(OTf)$_3$ in PhCN, taken by femtosecond laser excitation at 410 nm. b) Time profile of absorbance at 670 nm; inset: Time profiles at the shorter time range at 590 and 760 nm. The solid curve represents the best fit to the exponential rise or decay.

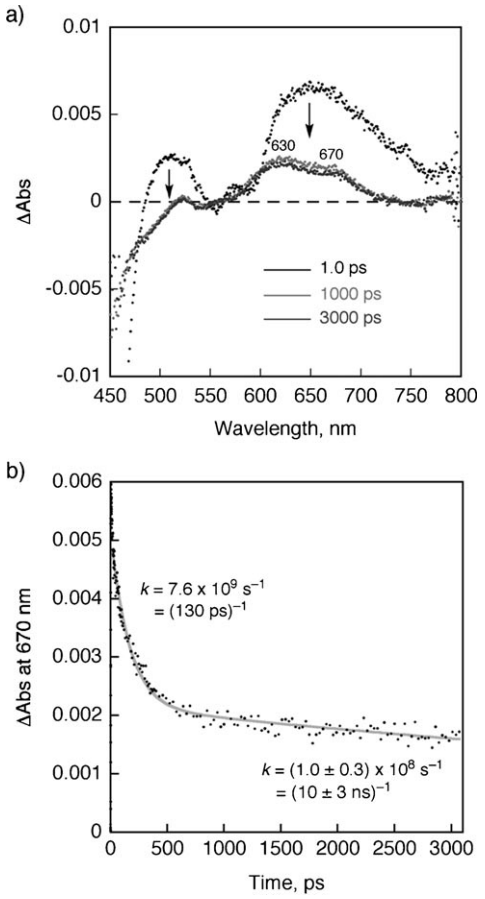

Figure 10. a) Transient absorption spectra of ZnPQ–AuPQ$^+$ in the presence of Sc(OTf)$_3$ (5.0 mM) in PhCN, taken by femtosecond laser excitation at 410 nm. b) Time profile of absorbance at 670 nm. The gray curve represents the best fit to the two-exponential decay.

at 1000 ps after femtosecond laser excitation agree well with what is observed in the one-electron oxidation of ZnPQ in the presence of Sc^{3+} (Supporting Information S4b). These absorption bands assigned to ZnPQ$^{\bullet+}$/$(Sc^{3+})_2$ are clearly blue-shifted as compared to those of ZnPQ$^{\bullet+}$ without Sc^{3+}. Since two Sc^{3+} ions bind to the ZnPQ and AuPQ moieties and the site of the electron-transfer reduction is changed from Au^{III} to PQ in AuPQ$^+$ (vide supra), photoinduced electron transfer from ^{1}ZnPQ*/$(Sc^{3+})_2$ to AuPQ$^+$/$(Sc^{3+})_2$ occurs to afford the CS state, ZnPQ$^{\bullet+}$/$(Sc^{3+})_2$–AuPQ$^{\bullet}$/$(Sc^{3+})_2$.

The time profile of absorbance at 670 nm prior to the back electron transfer in the presence of Sc^{3+} has two components (Figure 10b). The fast component with the rate constant of 7.6×10^9 s^{-1} (lifetime of 130 ps) corresponds to the electron transfer from ^{1}ZnPQ*/$(Sc^{3+})_2$ to AuPQ$^+$/$(Sc^{3+})_2$ to afford the CS state, ZnPQ$^{\bullet+}$/$(Sc^{3+})_2$–Au^{III}PQ$^{\bullet}$/$(Sc^{3+})_2$. The slow component with the rate $(1.0\pm0.3)\times10^8$ s^{-1} (lifetime of 10 ± 3 ns) corresponds to the electron transfer from ZnPQ/$(Sc^{3+})_2$ to ^{3}AuPQ$^+$*/$(Sc^{3+})_2$ to afford the CS state. The rate of electron transfer from ZnPQ to ^{3}AuPQ$^+$* is decelerated by three orders of magnitude after addition of Sc^{3+}. The decay of the CS state could not be determined because the limit of time range of our femtosecond laser flash photolysis is within 3.2 ns (see Experimental Section). This was determined by nanosecond laser flash photolysis (vide infra).

No transient absorption was observed by nanosecond laser flash photolysis of ZnPQ-AuPQ$^+$ in PhCN, because the photoinduced event is completely finished in the femto- to nanosecond timescale. In the presence of Sc^{3+}, however, a transient absorption spectrum is observed by nanosecond laser flash photolysis of ZnPQ–AuPQ$^+$ in PhCN, as shown in Figure 11.

The transient absorption maxima at 630 and 670 nm are the same as those observed at 3000 ns after femtosecond laser excitation in Figure 10a. This clearly indicates that the CS state is still observed by nanosecond laser flash photolysis of ZnPQ–AuPQ$^+$ in the presence of Sc^{3+} in PhCN.

The CS lifetime is determined from the single exponential decay of transient absorption to be 430 ns (Figure 12). Thus, the addition of Sc^{3+} to a solution of ZnPQ–AuPQ$^+$ in PhCN results in a 1700 times longer CS lifetime. Such remarkable elongation of the CS lifetime by the binding of Sc^{3+} to the PQ$^{\bullet-}$ moiety of the CS state can be explained by

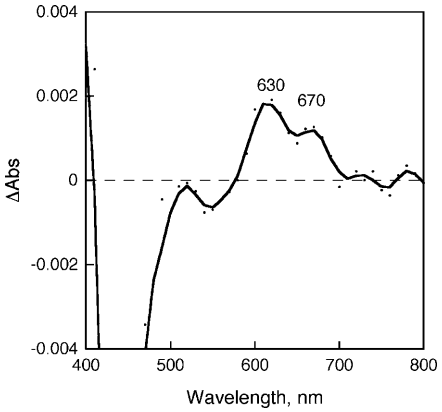

Figure 11. Transient absorption spectrum of ZnPQ–AuPQ$^+$ (1.0×10^{-5} M) in the presence of Sc^{3+} (5.0×10^{-3} M) in PhCN at 150 ns taken by nanosecond laser excitation at 430 nm.

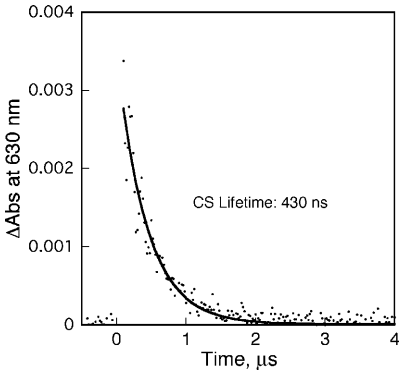

Figure 12. Decay time profile at 630 nm due to the CS state of ZnPQ–AuPQ$^+$ in the presence of Sc^{3+} in PhCN. The solid curve represents the best fit to the exponential decay.

the change in driving force of the back electron transfer and reorganization energy of the electron transfer, as shown in the energy diagrams of Scheme 2 in which the energies and photodynamics described above are summarized a) in the absence of Sc^{3+} and b) in the presence of Sc^{3+}. The energies of the singlet excited states of ZnPQ-AuPQ$^+$ in the absence and presence of Sc^{3+} were determined by using the absorption and fluorescence maxima of the corresponding reference compounds.

The triplet energies were determined by using phosphorescence in EPA with ethyl iodide glass at 77 K (see Experimental Section). The CS energies were determined from the difference in the redox potentials (vide supra). The stronger binding of Sc^{3+} to the PQ moiety following photoinduced electron transfer from ZnPQ to AuPQ$^+$ in PhCN results in a lowering of the CS state energy (Scheme 2b) as compared to the CS energy in the absence of Sc^{3+} (Scheme 2a). Since the initial one-electron oxidation potential of ZnPQ is shifted by only 40 mV due to the binding of Sc^{3+} to the quinoxaline moiety of ZnPQ (see the Supporting Information Figure S5), the large stabilization of the CS state mainly results from the large positive shift of the one-electron reduction

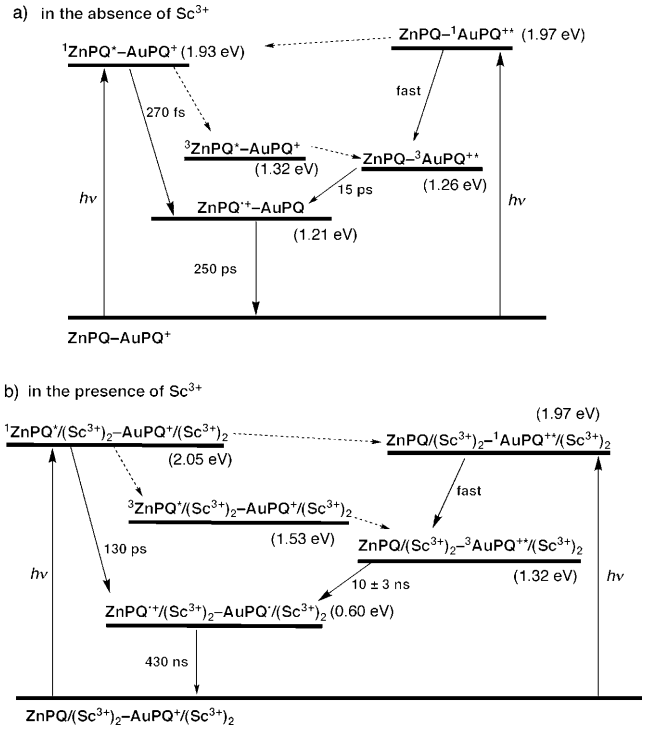

Scheme 2. Energy diagrams of photoinduced electron transfer in ZnPQ–AuPQ$^+$ in the a) absence and b) presence of $Sc(OTf)_3$. Solid arrows denote main pathways. Broken arrows denote minor pathways.

potential of the quinoxaline moiety by binding of Sc^{3+} (Figure 7), which causes the change in the site of electron transfer from the Au^{III} center to the quinoxaline moiety. Such a process is known to require a large reorganization energy. The lowering of the CS state energy due to the strong binding of Sc^{3+} to the $PQ^{\bullet-}$ moiety together with a large reorganization energy results in slower back electron transfer as well as photoinduced electron transfer in the Marcus normal region. Thus, the photodynamics of ZnPQ–AuPQ$^+$ are remarkably changed by binding of Sc^{3+} to the quinoxaline moiety of ZnPQ–AuPQ$^+$. The stronger binding of Sc^{3+} to the one-electron reduced quinoxaline moiety results in significant stabilization of the CS state and an increase in the reorganization energy of electron transfer, leading to remarkable lengthening of the CS lifetime.

Conclusions

The site of the first electron-transfer reduction in AuPQ and AuQPQ is changed from the Au^{III} center to the quinoxaline part of the PQ and QPQ macrocycles in PhCN containing Sc^{3+}, because of the strong binding of two and four Sc^{3+} ions to the two and four nitrogen sites of $PQ^{\bullet-}$ and $QPQ^{\bullet-}$, respectively. The photodynamics of an electron donor–acceptor linked compound (ZnPQ–AuPQ$^+$) are also changed drastically, particularly in terms of the CS state lifetime, which is 1700 times longer due to the strong binding of Sc^{3+} to $PQ^{\bullet-}$. Such a remarkable elongation of the CS lifetime in

the presence of Sc^{3+} provides a promising new strategy to lengthen the CS state of electron donor–acceptor ensembles, potentially proving useful in a number of areas, including photovoltaic devices.

Experimental Section

Chemicals: Scandium triflate ($Sc(OTf)_3$), ferrocene (Fc), 1,1′-dimethylferrocene (Me_2Fc), and decamethylferrocene (Fc*) were purchased from Aldrich and used as received without further purification. Benzonitrile (PhCN), obtained from Tokyo Chemical Industry or Aldrich was distilled over phosphorous pentaoxide (P_2O_5) under vacuum prior to use. Tetra-*n*-butylammonium hexafluorophosphate ($TBAPF_6$) was purchased from Sigma Chemical or Fluka Chemika, was recrystallized from ethyl alcohol, and was dried under vacuum at 40 °C for at least one week prior to use. The synthesis of 1-benzyl-1,4-dihydronicotinamide dimer $(BNA)_2$ was reported previously.[41] Synthesis of ZnPQ, $[AuPQ]PF_6$, and the dyad $[ZnPQ–AuPQ]PF_6$ are reported in the literature.[42] The synthesis of $[AuQPQ]PF_6$ is reported below. The reduced metal complexes of PQ were prepared by reduction with Fc* in the presence of $Sc(OTf)_3$.

Synthesis of hexafluorophosphate{5,10,15,20-tetrakis(3,5-di-*tert*-butylphenyl) bisquinoxalino[2,3-*b*′:12,13-*b*″]porphyrinato}aurate(III) ([AuQPQ]PF_6): General procedures for the synthesis of $[AuQPQ]PF_6$ are the same as those reported previously for other bisquinoxalinoporphyrins.[42] The ^{31}P NMR spectrum of the compound was acquired on a Bruker DPX-400 (162 MHz) spectrometer. ^{31}P NMR chemical shifts are referenced to external neat trimethyl phosphite, taken to be 140.85 ppm at room temperature.

5,10,15,20-Tetrakis(3,5-di-*tert*-butylphenyl)bisquinoxalino[2,3-*b*′:12,13-*b*″]porphyrin[41] (71.0 mg, 0.0560 mmol), potassium tetrachloroaurate(III) (105 mg, 0.278 mmol), and sodium acetate (170 mg, 2.17 mmol) were dissolved in a mixture of toluene (13 mL) and glacial acetic acid (18 M, 13 mL). The reaction mixture was heated at reflux for 4 h. The mixture was then diluted in dichloromethane (30 mL), washed with water (2× 100 mL), sodium carbonate solution (10%, 2×100 mL), and water (2× 100 mL), dried over anhydrous sodium sulfate, and filtered; the filtrate was evaporated to dryness. The residue was dissolved in chloroform (12 mL) and stirred with a saturated solution of potassium hexafluorophosphate (1.20 g, 6.52 mmol) in water (12 mL) for 18 h. The mixture was then diluted in chloroform (40 mL), washed with water (2×200 mL), dried over anhydrous sodium sulfate, and filtered; the filtrate was evaporated to dryness. The mixture was then purified by column chromatography over silica (chloroform/methanol; 100:4). The polar green band was collected and the solvent removed. The product was redissolved in chloroform (10 mL), and stirred with a saturated solution of potassium hexafluorophosphate (1.00 g, 5.43 mmol) in water (10 mL) for 18 h. The mixture was then washed with water (2×200 mL), dried over anhydrous sodium sulfate, and filtered; the filtrate was evaporated to dryness. The major green band was collected and the solvent was removed to afford pure $[AuQPQ]PF_6$ (20.0 mg, 22%) as a green solid. M.p. >300 °C; IR ($CHCl_3$): $\tilde{\nu}$ = 3059 (w), 2964 (s), 2905 (m), 2868 (m), 1595 (s), 1491 (w), 1477 (m), 1466 (w), 1421 (w), 1364 (s), 1329 (w), 1265 (m), 1248 (m), 1223 (s), 1217 (s), 1207 (m), 1136 (w), 1122 cm^{-1} (m); UV/Vis ($CHCl_3$): λ (log ε) = 345 sh (4.53), 384 (4.65), 451 (5.18), 537 (4.02), 601 (4.09), 644 nm (4.35); ^1H NMR (400 MHz, $CDCl_3$, 25 °C, TMS): δ = 1.49 (s, 72H; *tert*-butyl H), 7.94 (d, J = 1.8 Hz, 8H; H_o), 7.95–7.96 (m, 8H; quinoxaline H), 8.015 (t, J = 1.8 Hz, 4H; H_p), 9.36 ppm (s, 4H; β-pyrrolic H); ^{31}P NMR (162 MHz, $CDCl_3$): δ = −146.42 (septet, J = 714 Hz, 1P, PF_6); MS (ESI): *m/z*: 1462.0 ($[M-PF_6]^+$ requires 1461.7); HR-ESI-FT/ICR: *m/z*: $[M-PF_6]^+$ 1461.7408; $C_{88}H_{96}AuF_6N_8P$ requires 1461.7418.

Instrumentation: Spectral measurements were performed using a Hewlett Packard 8453 diode array spectrophotometer. ESR measurements were recorded on a JEOL JES-RE1XE spectrometer. Cyclic voltammetry was performed on either an ALS electrochemical analyzer or an EG&G Princeton Applied Research (PAR) 173 potentiostat/galvanostat in deaerated PhCN, 0.1 M $TBAPF_6$ using a conventional three-electrode cell. The working electrode was a glassy carbon electrode, the counter electrode was a Pt wire, and the reference was either a commercially available or homemade SCE. The homemade SCE was separated from the bulk of the solution by a fritted glass bridge of low porosity that contained PhCN, 0.1 M $TBAPF_6$. UV/Vis spectroelectrochemical experiments were performed with a homemade thin-layer cell with a platinum net working electrode. Time-resolved UV/Vis spectra were recorded with a Hewlett Packard 8453 diode array spectrophotometer. Phosphorescence spectra were measured in a deaerated EPA/ethyl iodide (5:5:2:12 isopentane: diethyl ether: ethanol: ethyl iodide) glass at 77 K. Near-IR emission spectra of singlet oxygen were recorded on a SPEX Fluorolog τ3 spectrophotometer. A photomultiplier (Hamamatsu Photonics, R5509–72) was used to detect emission in the near-infrared region (band path 2 mm).

Laser flash photolysis: Time-resolved fluorescence decays were measured by a Photon Technology International GL-3300 with a Photon Technology International GL-302, nitrogen laser/pumped dye laser system, equipped with a four channel digital delay/pulse generator (Stanford Research System Inc. DG535) and a motor driver (Photon Technology International MD-5020). The excitation wavelength was 431 nm using POPOP (Wako Pure Chemical Ind. Ltd., Japan) as a dye. Fluorescence lifetimes were determined by an exponential curve fit using a microcomputer.

Femtosecond transient absorption spectroscopy experiments were conducted using an ultrafast source: Integra-C (Quantronix Corp.), an optical parametric amplifier: TOPAS (Light Conversion Ltd.) and a commercially available optical detection system: Helios provided by Ultrafast Systems LLC. The source for the pump and probe pulses were derived from the fundamental output of Integra-C (780 nm, 2 mJ/pulse and fwhm = 130 fs) at a repetition rate of 1 kHz. 75% of the fundamental output of the laser was introduced into TOPAS, which has optical frequency mixers, resulting in a tunable range from 285 to 1660 nm, with the rest of the output used for white light generation. Prior to generating the probe continuum, a variable neutral density filter was inserted in the path in order to generate a stable continuum, then the laser pulse was fed to a delay line that provides an experimental time window of 3.2 ns with a maximum step resolution of 7 fs. In our experiments, a wavelength at 410 nm of TOPAS output, which is the fourth harmonic of signal or idler pulses, was chosen as the pump beam. As this TOPAS output consists of not only the desirable wavelength but also unnecessary wavelengths, the latter were filtered using a wedge prism with a wedge angle of 18°. The desirable beam was irradiated at the sample cell with a spot size of 1 mm diameter, where it was merged with the white probe pulse in a close angle (< 10°). The probe beam, after passing through the 2 mm sample cell, was focused on a fiber optic cable that was connected to a CCD spectrograph for recording the time-resolved spectra (410–800 nm). Typically, 2500 excitation pulses were averaged for 5 s to obtain the transient spectrum at a set delay time. Kinetic traces at appropriate wavelengths were assembled from the time-resolved spectral data. All measurements were conducted at room temperature, 295 K.

For nanosecond laser flash photolysis experiments, deaerated solutions of the dyad were excited by a Panther OPO equipped with a Nd:YAG laser (Continuum, SLII-10, 4–6 ns fwhm) at λ = 430 nm with a power of 10 mJ per pulse. The photochemical reactions were monitored by continuous exposure to a Xe lamp (150 W) as a probe light and a photomultiplier tube (Hamamatsu 2949) as a detector. The transient spectra were recorded using fresh solutions in each laser excitation. The solution was deoxygenated by argon purging for 15 min prior to the measurements.

Theoretical calculations: Density functional calculations were performed with Gaussian 03[43] using the spin-restricted B3LYP functional[44] on an 8-process Quantum Cube™ developed by the Parallel Quantum Solutions. All calculations were performed using GAUSSIAN-03. Graphical outputs of the computational results were generated with the Gauss View software program (version 3.09) developed by Semichem, Inc.[45]

Acknowledgements

This work was partially supported by the Ministry of Education, Culture, Sports, Science and Technology of Japan, with a Grant-in-Aid (Nos. 19205019, 19750034, 21750146) to S.F. and K.O. and a Global COE program, "The Global Education and Research Center for Bio-Environmental Chemistry" to S.F. and KOSEF/MEST through WCU project (R31-2008-000-10010-0). The support of the Robert A. Welch Foundation (KMK, Grant E-680) and the Texas Advanced Research Program to K.M.K. under Grant No. 003652-0018-2001 and from the Rice-Houston Alliance for Graduate Education and Professoriate for Minorities are also gratefully acknowledged. This work was also partially supported by a Discovery Research Grant from the Australian Research Counci (DP0208776) to M.J.C.

[1] *The Photosynthetic Reaction Center* (Eds.: J. Deisenhofer, J. R. Norris), Academic Press, New York, **1993**.

[2] a) R. A. Marcus, *Angew. Chem.* **1993**, *105*, 1161–1172; *Angew. Chem. Int. Ed. Engl.* **1993**, *32*, 1111–1121; b) R. A. Marcus, N. Sutin, *Biochim. Biophys. Acta Rev. Bioenerg.* **1985**, *811*, 265–322.

[3] a) M. R. Wasielewski, *Chem. Rev.* **1992**, *92*, 435–461; b) M. R. Wasielewski in *Photoinduced Electron Transfer, Part A* (Eds.: M. A. Fox, M. Chanon), Elsevier, Amsterdam, **1988**, pp. 161–206.

[4] a) D. Gust, T. A. Moore, A. L. Moore in *Electron Transfer in Chemistry, Vol. 3* (Ed.: V. Balzani), Wiley-VCH, Weinheim, **2001**, pp. 272—336; b) D. Gust, T. A. Moore in *The Porphyrin Handbook, Vol. 8* (Eds.: K. M. Kadish, K. M. Smith, R. Guilard), Academic Press, Burlington, **2000**, pp. 153–190; c) D. Gust, T. A. Moore, A. L. Moore, *Acc. Chem. Res.* **2001**, *34*, 40–48.

[5] a) M. N. Paddon-Row, *Acc. Chem. Res.* **1994**, *27*, 18–25; b) K. D. Jordan, M. N. Paddon-Row, *Chem. Rev.* **1992**, *92*, 395–410.

[6] a) S. Fukuzumi, D. M. Guldi in *Electron Transfer in Chemistry, Vol. 2* (Ed.: V. Balzani), Wiley-VCH, Weinheim, **2001**, pp. 270—337; b) D. M. Guldi, *Chem. Commun.* **2000**, 321–327; c) D. M. Guldi, M. Prato, *Acc. Chem. Res.* **2000**, *33*, 695–703; d) D. M. Guldi, *Chem. Soc. Rev.* **2002**, *31*, 22–36; e) L. Sánchez, N. Martin, D. M. Guldi, *Angew. Chem.* **2005**, *117*, 5508–5516; *Angew. Chem. Int. Ed.* **2005**, *44*, 5374–5382; f) I. Bouamaied, T. Coskun, E. Stulz in *Non-Covalent Multi-Porphyrin Assemblies* (Ed.: E. Alessio), Springer, Berlin, **2006**, pp. 1–47.

[7] a) H. Imahori, K. Tamaki, D. M. Guldi, C. Luo, M. Fujitsuka, O. Ito, Y. Sakata, S. Fukuzumi, *J. Am. Chem. Soc.* **2001**, *123*, 2607–2617; b) H. Imahori, D. M. Guldi, K. Tamaki, Y. Yoshida, C. Luo, Y. Sakata, S. Fukuzumi, *J. Am. Chem. Soc.* **2001**, *123*, 6617–6628; c) H. Imahori, Y. Sekiguchi, Y. Kashiwagi, T. Sato, Y. Araki, O. Ito, H. Yamada, S. Fukuzumi, *Chem. Eur. J.* **2004**, *10*, 3184–3196; d) H. Imahori, S. Fukuzumi, *Adv. Funct. Mater.* **2004**, *14*, 525–536.

[8] a) S. Fukuzumi, H. Kotani, K. Ohkubo, S. Ogo, N. V. Tkachenko, H. Lemmetyinen, *J. Am. Chem. Soc.* **2004**, *126*, 1600–1601; b) K. Ohkubo, H. Kotani, S. Fukuzumi, *Chem. Commun.* **2005**, 4520–4522; c) S. Fukuzumi, H. Kotani, K. Ohkubo, *Phys. Chem. Chem. Phys.* **2008**, *10*, 5159–5162; d) A. Harriman, *Angew. Chem.* **2004**, *116*, 5093–5095; *Angew. Chem. Int. Ed.* **2004**, *43*, 4985–4987; e) M. Tanaka, K. Ohkubo, C. P. Gros, R. Guilard, S. Fukuzumi, *J. Am. Chem. Soc.* **2006**, *128*, 14625–14633.

[9] a) F. D'Souza, O. Ito, *Coord. Chem. Rev.* **2005**, *249*, 1410–1422; b) M. E. El-Khouly, O. Ito, P. M. Smith, F. D'Souza, *J. Photochem. Photobiol. C* **2004**, *5*, 79–104; c) R. Chitta, F. D'Souza, *J. Mater. Chem.* **2008**, *18*, 1440–1471.

[10] a) S. Fukuzumi, *Phys. Chem. Chem. Phys.* **2008**, *10*, 2283–2297; b) S. Fukuzumi, T. Kojima, *J. Mater. Chem.* **2008**, *18*, 1427–1439; c) K. Ohkubo, S. Fukuzumi, *J. Porphyrins Phthalocyanines* **2008**, *12*, 993–1004; d) K. Ohkubo, S. Fukuzumi, *Bull. Chem. Soc. Jpn.* **2009**, *82*, 303–315.

[11] a) S. Fukuzumi in *Electron Transfer in Chemistry, Vol. 4* (Ed.: V. Balzani), Wiley-VCH, Weinheim, **2001**, pp. 3–67; b) S. Fukuzumi, S. Itoh, in *Advances in Photochemistry,Vol. 25* (Eds.: D. C. Neckers, D. H. Volman, G. von Bünau), Wiley, New York, **1998**, pp. 107–172.

[12] a) S. Fukuzumi, *Bull. Chem. Soc. Jpn.* **1997**, *70*, 1–28; b) S. Fukuzumi, *Org. Biomol. Chem.* **2003**, *1*, 609–620; c) S. Fukuzumi, *Bull. Chem. Soc. Jpn.* **2006**, *79*, 177–195.

[13] a) S. Fukuzumi, K. Okamoto, H. Imahori, *Angew. Chem.* **2002**, *114*, 642–644; *Angew. Chem. Int. Ed.* **2002**, *41*, 620–622; b) S. Fukuzumi, K. Okamoto, Y. Yoshida, H. Imahori, Y. Araki, O. Ito, *J. Am. Chem. Soc.* **2003**, *125*, 1007–1013; c) K. Okamoto, H. Imahori, S. Fukuzumi, *J. Am. Chem. Soc.* **2003**, *125*, 7014–7021; d) K. Okamoto, Y. Araki, O. Ito, S. Fukuzumi, *J. Am. Chem. Soc.* **2004**, *126*, 56–57; e) K. Okamoto, Y. Mori, H. Yamada, H. Imahori, S. Fukuzumi, *Chem. Eur. J.* **2004**, *10*, 474–483.

[14] a) S. Fukuzumi, K. Ohkubo, J. Ortiz, A. M. Gutiérrez, F. Fernández-Lázaro, Á. Sastre-Santos, *Chem. Commun.* **2005**, 3814–3816; b) S. Fukuzumi, K. Ohkubo, J. Ortiz, A. M. Gutiérrez, F. Fernández-Lázaro, Á. Sastre-Santos, *J. Phys. Chem. A* **2008**, *112*, 10744–10752.

[15] a) S. Fukuzumi, K. Ohkubo, *Chem. Eur. J.* **2000**, *6*, 4532–4535; b) S. Fukuzumi, K. Ohkubo, *J. Am. Chem. Soc.* **2002**, *124*, 10270–10271.

[16] a) J. Yuasa, T. Suenobu, S. Fukuzumi, *ChemPhysChem* **2006**, *7*, 942–954; b) J. Yuasa, S. Yamada, S. Fukuzumi, *J. Am. Chem. Soc.* **2006**, *128*, 14938–14948; c) J. Yuasa, S. Yamada, S. Fukuzumi, *Chem. Eur. J.* **2008**, *14*, 1866–1874.

[17] a) S. Fukuzumi, J. Yuasa, N. Satoh, T. Suenobu, *J. Am. Chem. Soc.* **2004**, *126*, 7585–7594; b) S. Fukuzumi, K. Ohkubo, T. Okamoto, *J. Am. Chem. Soc.* **2002**, *124*, 14147–14155; c) J. Yuasa, T. Suenobu, S. Fukuzumi, *J. Am. Chem. Soc.* **2003**, *125*, 12090–12091; d) K. Ohkubo, J. Ortiz, L. Martín-Gomis, F. Fernández-Lázaro, Á. Sastre-Santos, S. Fukuzumi, *Chem. Commun.* **2007**, 589–591.

[18] a) S. Fukuzumi, H. Mori, H. Imahori, T. Suenobu, Y. Araki, O. Ito, K. M. Kadish, *J. Am. Chem. Soc.* **2001**, *123*, 12458–12465; b) S. Fukuzumi, Y. Fujii, T. Suenobu, *J. Am. Chem. Soc.* **2001**, *123*, 10191–10199.

[19] S. Fukuzumi, K. Ohkubo, W. Zhu, M. Sintic, T. Khoury, P. J. Sintic, W. E. Z. Ou, M. J. Crossley, K. M. Kadish, *J. Am. Chem. Soc.* **2008**, *130*, 9451–9458.

[20] W. E. K. M. Kadish, P. J. Sintic, T. Khoury, L. J. Govenlock, Z. Ou, J. Shao, K. Ohkubo, J. R. Reimers, S. Fukuzumi, M. J. Crossley, *J. Phys. Chem. A* **2008**, *112*, 556–570.

[21] K. M. Kadish, W. E. Z. Ou, J. Shao, P. J. Sintic, K. Ohkubo, S. Fukuzumi, M. J. Crossley, *Chem. Commun.* **2002**, 356–357.

[22] Z. Ou, K. M. Kadish, W. E. J. Shao, P. J. Sintic, K. Ohkubo, S. Fukuzumi, M. J. Crossley, *Inorg. Chem.* **2004**, *43*, 2078–2086.

[23] a) T. Shimidzu, T. Iyoda, H. Segawa, K. Honda, *Nouv. J. Chim.* **1986**, *10*, 213; b) T. Shimidzu, H. Segawa, T. Iyoda, K. Honda, *J. Chem. Soc. Faraday Trans. 2* **1987**, *83*, 2191–2200.

[24] M. E. Jamin, R. T. Iwamoto, *Inorg. Chim. Acta* **1978**, *27*, 135–143.

[25] A. Antipas, D. Dolphin, M. Gouterman, E. C. Johnson, *J. Am. Chem. Soc.* **1978**, *100*, 7705–7709.

[26] a) K. M. Kadish, W. E. P. J. Sintic, Z. Ou, J. Shao, K. Ohkubo, S. Fukuzumi, L. J. Govenlock, J. A. McDonald, A. C. Try, Z. L. Cai, J. R. Reimers, M. J. Crossley, *J. Phys. Chem. B* **2007**, *111*, 8762–8774; b) Z. Ou, W. E. J. Shao, P. L. Burn, C. S. Sheehan, R. Walton, K. M. Kadish, M. J. Crossley, *J. Porphyrins Phthalocyanines* **2005**, *9*, 142–151.

[27] a) S. Fukuzumi, K. Ohkubo, W. E. Z. Ou, J. Shao, K. M. Kadish, J. A. Hutchison, K. P. Ghiggino, P. J. Sintic, M. J. Crossley, *J. Am. Chem. Soc.* **2003**, *125*, 14984–14985; b) K. Ohkubo, P. J. Sintic, N. V. Tkachenko, H. Lemmetyinen, W. E. Z. Ou, J. Shao, K. M. Kadish, M. J. Crossley, S. Fukuzumi, *Chem. Phys.* **2006**, *326*, 3–14; c) J. A. Hutchison, P. J. Sintic, M. J. Crossley, T. Nagamura, K. P. Ghiggino, *Phys. Chem. Chem. Phys.* **2009**, *11*, 3478–3489.

[28] a) J. Wiberg, L. Guo, K. Pettersson, D. Nilsson, T. Ljungdahl, J. Mårtensson, B. Albinsson, *J. Am. Chem. Soc.* **2007**, *129*, 155–163; b) T. Ljungdahl, K. Pettersson, B. Albinsson, J. Mårtensson, *J. Org. Chem.* **2006**, *71*, 1677–1687; c) M. P. Eng, T. Ljungdahl, J. Andréasson, J. Mårtensson, B. Albinsson, *J. Phys. Chem. A* **2005**, *109*, 1776–1784.

[29] L. Flamigni, F. Barigelletti, N. Armaroli, J.-P. Collin, I. M. Dixon, J.-P. Sauvage, J. A. G. Williams, *Coord. Chem. Rev.* **1999**, *190–192*, 671–682.

[30] a) M.-J. Blanco, M.-C. Jiménez, J.-C. Chambron, V. Heitz, M. Linke, J.-P. Sauvage, *Chem. Soc. Rev.* **1999**, *28*, 293–305; b) J.-C. Chambron, J.-P. Collin, J.-O. Dalbavie, C. O. Dietrich-Buchecker, V. Heitz, F. Odobel, N. Solladie, J.-P. Sauvage, *Coord. Chem. Rev.* **1998**, *178–180*, 1299–1312; c) A. Harriman, J.-P. Sauvage, *Chem. Soc. Rev.* **1996**, *25*, 41–48.

[31] a) I. M. Dixon, J.-P. Collin, J.-P. Sauvage, F. Barigelletti, L. Flamigni, *Angew. Chem.* **2000**, *112*, 1348–1351; *Angew. Chem. Int. Ed.* **2000**, *39*, 1292–1295; b) L. Flamigni, I. M. Dixon, J.-P. Collin, J.-P. Sauvage, *Chem. Commun.* **2000**, 2479–2480; c) M. Linke, J.-C. Chambron, V. Heitz, J.-P. Sauvage, S. Encinas, F. Barigelletti, L. Flamigni, *J. Am. Chem. Soc.* **2000**, *122*, 11834–11844; d) L. Flamigni, G. Marconi, I. M. Dixon, J.-P. Collin, J.-P. Sauvage, *J. Phys. Chem. B* **2002**, *106*, 6663–6671.

[32] a) A. Harriman, V. Heitz, J.-P. Sauvage, *J. Phys. Chem.* **1993**, *97*, 5940–5946; b) A. Harriman, F. Odobel, J.-P. Sauvage, *J. Am. Chem. Soc.* **1995**, *117*, 9461–9472.

[33] K.; Kilså, J. Kajanus, A. N. Marcpherson, J. Mårtensson, B. Albinsson, *J. Am. Chem. Soc.* **2001**, *123*, 3069–3080.

[34] L. Flamigni, F. Barigelletti, N. Armaroli, J.-P. Collin, J.-P. Sauvage, J. A. G. Williams, *Chem. Eur. J.* **1998**, *4*, 1744–1754.

[35] The large peak separation for the first reduction results from the slow electron transfer with the large reorganization energy of electron transfer due to the much stronger binding of Sc^{3+} to the reduced state. Similar behavior has been reported in reference [16a]. For an example of CV with a large reorganization energy, see: Y.-M. Lee, H. Kotani, T. Suenobu, W. Nam, S. Fukuzumi, *J. Am. Chem. Soc.* **2008**, *130*, 434–435.

[36] Large current in CV for the second reduction as compared with the others may result from partial chemical reaction of the two-electron reduced species of $AuPQ^{+}/(Sc^{3+})_2$ [$AuPQ^{-}/(Sc^{3+})_2$] such as disproportionation between two $AuPQ^{-}/(Sc^{3+})_2$ molecules to produce $AuPQ/(Sc^{3+})_2$ and $AuPQ^{2-}/(Sc^{3+})_2$.

[37] S. Fukuzumi, S. Mochizuki, T. Tanaka, *Inorg. Chem.* **1989**, *28*, 2459–2465.

[38] S. Fukuzumi, K. Okamoto, C. P. Gros, R. Guilard, *J. Am. Chem. Soc.* **2004**, *126*, 10441–10449.

[39] The structural optimization of $AuPQ(Sc^{3+})_2$ was carried out by using UFF calculation. The binding site of Sc^{3+} has enough space due to the flexible PQ entity as shown in Figure S6.

[40] J. Andréasson, G. Kodis, S. Lin, A. L. Moore, T. A. Moore, D. Gust, J. Mårtensson, B. Albinsson, *Photochem. Photobiol.* **2002**, *76*, 47–50.

[41] S. Fukuzumi, T. Suenobu, M. Patz, T. Hirasaka, S. Itoh, M. Fujitsuka, O. Ito, *J. Am. Chem. Soc.* **1998**, *120*, 8060–8068.

[42] M. J. Crossley, P. J. Sintic, R. Walton, J. R. Reimers, *Org. Biomol. Chem.* **2003**, *1*, 2777–2787.

[43] Gaussian 03 (Revision C.02), M. J. Frisch, G. W. Trucks, H. B. Schlegel, G. E. Scuseria, M. A. Robb, J. R. Cheeseman, J. A. Montgomery Jr., T. Vreven, K. N. Kudin, J. C. Burant, J. M. Millam, S. S. Iyengar, J. Tomasi, V. Barone, B. Mennucci, M. Cossi, G. Scalmani, N. Rega, G. A. Petersson, H. Nakatsuji, M. Hada, M. Ehara, K. Toyota, R. Fukuda, J. Hasegawa, M. Ishida, T. Nakajima, Y. Honda, O. Kitao, H. Nakai, M. Klene, X. Li, J. E. Knox, H. P. Hratchian, J. B. Cross, C. Adamo, J. Jaramillo, R. Gomperts, R. E. Stratmann, O. Yazyev, A. J. Austin, R. Cammi, C. Pomelli, J. W. Ochterski, P. Y. Ayala, K. Morokuma, G. A. Voth, P. Salvador, J. J. Dannenberg, V. G. Zakrzewski, S. Dapprich, A. D. Daniels, M. C. Strain, O. Farkas, D. K. Malick, A. D. Rabuck, K. Raghavachari, J. B. Foresman, J. V. Ortiz, Q. Cui, A. G. Baboul, S. Clifford, J. Cioslowski, B. B. Stefanov, G. Liu, A. Liashenko, P. Piskorz, I. Komaromi, R. L. Martin, D. J. Fox, T. Keith, M. A. Al-Laham, C. Y. Peng, A. Nanayakkara, M. Challacombe, P. M. W. Gill, B. Johnson, W. Chen, M. W. Wong, C. Gonzalez, J. A. Pople, Gaussian, Inc., Pittsburgh, PA, 2004.

[44] A. D. Becke, *J. Chem. Phys.* **1993**, *98*, 5648–5652.

[45] Gaussview, R. Dennington II, T. Keith, J. Millam, K. Eppinnett, W. L. Hovell, R. Gilliland, Semichem, Inc., Shawnee Mission, **2003**.

Received: April 27, 2009
Published online: August 26, 2009

